Phonons from Powder Diffraction: A Quantitative Model-Independent Evaluation

Andrew L. Goodwin,[1] Matthew G. Tucker,[1] Martin T. Dove,[1,*] and David A. Keen[2,3]

[1]*Department of Earth Sciences, Cambridge University, Downing Street, Cambridge CB2 3EQ, United Kingdom*
[2]*Department of Physics, Oxford University, Clarendon Laboratory, Parks Road, Oxford OX1 3PU, United Kingdom*
[3]*ISIS Facility, Rutherford Appleton Laboratory, Chilton, Didcot, Oxfordshire OX11 0QX, United Kingdom*

(Received 30 March 2004; published 12 August 2004)

We describe a model-independent approach for the extraction of detailed lattice dynamics information from neutron powder diffraction data, based on a statistical analysis of atomistic configurations generated using reverse Monte Carlo structural refinement. Phonon dispersion curves for MgO extracted in this way are shown to reproduce many of the important features found in those determined independently using neutron triple-axis spectroscopy. By means of molecular dynamics simulations, we quantify the extent to which the diffraction data are sensitive to lattice dynamics in this system.

DOI: 10.1103/PhysRevLett.93.075502 PACS numbers: 63.20.–e, 61.12.Bt

Many physical properties of crystalline materials can be understood in terms of the effects of atomic vibrational motion on macroscopic behavior; examples include thermal expansion, heat capacity, thermal conductivity, displacive and magnetic phase transitions, and superconductivity. The established methods of investigating the phonons that describe such motion are inelastic neutron scattering (INS) and, more recently, high energy resolution inelastic x-ray scattering (IXS) experiments [1,2]. These can yield information on the energies of phonon modes along particular symmetry directions in the Brillouin zone (BZ). However, they are intensity limited (and hence time consuming) and rely upon the availability of single crystals. For systems where single-crystal samples of sufficient size are unavailable, INS and IXS experiments can yield only information integrated over the BZ. Consequently, there is significant interest in the development of alternative methods for obtaining detailed dynamics information from crystalline powder samples. In particular, the use of neutron powder diffraction (NPD) data to extract phonon dispersion curves is a particularly attractive approach and one that has received recent attention [3–6]. The appeal lies in the relative ease with which NPD experiments can be performed; unlike INS/IXS triple-axis spectroscopy, they do not require single-crystal samples and are (by comparison) versatile, time efficient, and inexpensive.

The observed scattering function $S(Q)$ contains all the lattice dynamics information, but the quality of this information is degraded through the integration over dynamical and directional degrees of freedom performed in powder diffraction experiments. Recent attempts to quantify the amount of dynamics information preserved in this procedure [3–6] have focused upon analysis of the pair distribution function (PDF), which can be derived by direct Fourier transform of $S(Q)$. Refinement of parameters in standard phonon models by comparison of their associated PDFs with those obtained by NPD experiments has been shown [5] to reproduce phonon dispersion curves to within a few percent accuracy for some very simple systems such as fcc Ni, fcc Ag and bcc Fe. Materials requiring more complex dynamical models have proved to be a stumbling block for this approach.

In this Letter, we describe a novel method of directly probing the dynamics information held within the PDF (and similar diffraction-derived data) without constraining the results in terms of some form of imposed phonon model. Such an approach is intrinsically more general and is likely to indicate the true limitations of NPD as a means of obtaining dynamics information. Moreover, the need to select an appropriate phonon model *a priori* is avoided. This is of particular importance in systems for which INS/IXS studies are impractical (due to the unavailability of sufficiently large single crystals, for example), where a suitable model may not be known.

A recent study [7] illustrated that the relevant analysis of reverse Monte Carlo (RMC) configurations of α-quartz and β-quartz, generated by fitting to NPD data, was able to reproduce detailed single-crystal diffuse scattering patterns. The structure of such scattering is a direct manifestation of phonons. Consequently, we were optimistic that RMC might prove to be a suitable probe for investigating the extent of dynamics information accessible from NPD data [8].

Our approach involved using the RMC procedure to generate a large number of independent atomistic configurations consistent with experimental NPD data. The procedure, which is described in detail elsewhere [9], involves minimization of the "energy" function

$$\chi^2_{\mathrm{RMC}} = \chi^2_{S(Q)} + \chi^2_{T(r)} + \chi^2_{\mathrm{Bragg}}, \tag{1}$$

where

$$\chi^2_{S(Q)} = \sum_k \sum_j [S_{\mathrm{calc}}(Q_j)_k - S_{\mathrm{exp}}(Q_j)_k]^2/\sigma^2_k(Q_j),$$

$$\chi^2_{T(r)} = \sum_j [T_{\mathrm{calc}}(r_j) - T_{\mathrm{exp}}(r_j)]^2/\sigma^2(r_j),$$

$$\chi^2_{\mathrm{Bragg}} = \sum_{h,k,l} [I_{\mathrm{calc}}(hkl) - I_{\mathrm{exp}}(hkl)]^2/\sigma^2(hkl). \tag{2}$$

 © 2004 The American Physical Society

Here, $T(r)$ is the radial distribution function and is similar to the PDF [10], and $\chi^2_{S(Q)}$ includes contributions by each of k data sets. Refinement of the Bragg intensities $I(hkl)$ is included as they provide information on mean square displacements of atoms, which complements the widths of the peaks in the PDF [and, hence, $T(r)$]. Each configuration derived in this manner corresponds to a static "snapshot" of a supercell of atoms within the sample. The size of these configurations is limited only by the available computational resources and quality of data. Importantly, these configurations are not unique. Each is equally consistent with the data, irrespective of the differences in their local atomic displacements. In this way, the ensemble of configurations can be thought of as a series of snapshots of the same set of atoms undergoing vibrational motion where each frame has been taken at a different point in time. There will be a unique set of phonons across the BZ (with resolution determined by the size of the supercell) that are capable of describing the vibrational motion in this way.

A method of extracting phonons from atomistic configurations has been described previously [11,12], where it was used to analyze output from molecular dynamics (MD) simulations. The method is equally applicable in the present instance. For each configuration, indexed by t (with reference to the concept of time introduced above), a number of collective variables of the form

$$U(\mathbf{k}, t) = \frac{1}{\sqrt{N}} \sum_j \sqrt{m_j}\, u_j(t) \exp(i\mathbf{k} \cdot \mathbf{R}_j) \qquad (3)$$

are calculated, where the sum is over all atoms of a particular type and $u_j(t)$ is the displacement of each atom j along one of the principal axes. There will be three of these variables for each atom in the (primitive) unit cell corresponding to each of the three principal axes. All $3Z$ collective variables (where Z is the number of atoms in the primitive unit cell) are assembled into a single column matrix $\mathbf{T}(\mathbf{k}, t)$, which can be related to the normal mode coordinate column vector $\mathbf{Q}(\mathbf{k}, t)$ by the equation:

$$\mathbf{Q}(\mathbf{k}, t) = \mathbf{A}(\mathbf{k}) \cdot \mathbf{T}(\mathbf{k}, t). \qquad (4)$$

This relation represents a change of basis between the normal coordinates (which form the basis for $\mathbf{Q}$) and the atom/direction coordinates (which form the basis for $\mathbf{T}$). As these bases are independent of t (i.e., they are the same for each configuration in our ensemble), the change of basis matrix $\mathbf{A}$ depends only on $\mathbf{k}$. We calculate the t-averaged matrix $\mathbf{S}$ by the relation:

$$\mathbf{S}(\mathbf{k}) = \langle \mathbf{T}(\mathbf{k}) \cdot \mathbf{T}^{\mathrm{T}}(-\mathbf{k}) \rangle. \qquad (5)$$

This is useful in exploiting the property that the basis of $\mathbf{Q}$ is the set of normal coordinates and hence the matrix $\mathbf{Q}(\mathbf{k}, t) \cdot \mathbf{Q}^{\mathrm{T}}(-\mathbf{k}, t)$ is diagonal. The uniqueness of diagonalization yields the elements of $\mathbf{Q}$ from $\mathbf{S}$:

$$\mathbf{A}(\mathbf{k}) \cdot \mathbf{S}(\mathbf{k}) \cdot \mathbf{A}^{\mathrm{T}}(\mathbf{k}) = \langle \mathbf{Q}(\mathbf{k}) \cdot \mathbf{Q}^{\mathrm{T}}(-\mathbf{k}) \rangle, \qquad (6)$$

and hence the mode frequencies:

$$\omega_i^2(\mathbf{k}) = \frac{k_{\mathrm{B}} T}{\langle Q(\mathbf{k}) \cdot Q^{\mathrm{T}}(-\mathbf{k}) \rangle_{i,i}}. \qquad (7)$$

Moreover, $\mathbf{A}$ contains the eigenvectors of $\mathbf{S}$ and so its elements describe the atomic motions characteristic of each phonon mode. In this way, the method yields both the frequencies and nature of the phonons at arbitrary wave vector.

We chose rocksalt-structured magnesium oxide (MgO) as an initial system with which to test the suitability of our approach as its lattice dynamics, although nontrivial, are well understood [13]. Neutron total scattering data were collected at room temperature on the GEM instrument at ISIS [14] over a range of momentum transfers $1 < Q < 42$ Å^{-1}. These data were then converted to $S(Q)$, $T(r)$, and Bragg intensity data. All three sets were used as input for the RMC procedure to generate 500 configurations, each containing a $10 \times 10 \times 10$ array of fcc unit cells. This ensemble was analyzed according to the method described above along the symmetry directions $[00\xi]$, $[01\xi]$, $[0\xi\xi]$, and $[\xi\xi\xi]$ at intervals of $1/5$ to yield the phonon dispersion curves illustrated in Fig. 1(b) [15]. Calculation of phonon frequencies at symmetry equivalent wave vectors enabled estimation of the errors associated with each measurement and we were able to assign the nature of each phonon branch by inspection of the corresponding eigenvectors. We restricted our attention to the above symmetry directions entirely for the sake of convention; in contrast to triple-axis INS experiments, our analysis allows convenient determination of phonon mode frequencies for all wave vectors within the BZ, limited only by the resolution of the box size.

It is important to emphasize that these results were recovered wholly from the NPD data; there is no reliance on an imposed phonon model. Consequently, it is not altogether surprising that their form does not match the INS-derived phonon dispersion curves perfectly [Fig. 1(a)]. The features are generally well preserved with surprising levels of detail discernible in the dispersion. In particular, splitting of the transverse modes along $[01\xi]$ and $[0\xi\xi]$ and the clear distinction between optic and acoustic modes are key features shared by both INS-derived and RMC-derived dispersion curves. In other respects, the curves are very different. The most noticeable of these differences is the absence of any splitting between the LO and TO bands at the zone center. This splitting, which arises as a result of the difference in long-range fields given by longitudinal and transverse modes as $\mathbf{k} \rightarrow 0$, is more or less implicit in any dynamical model that includes charge. On the other hand, it is a

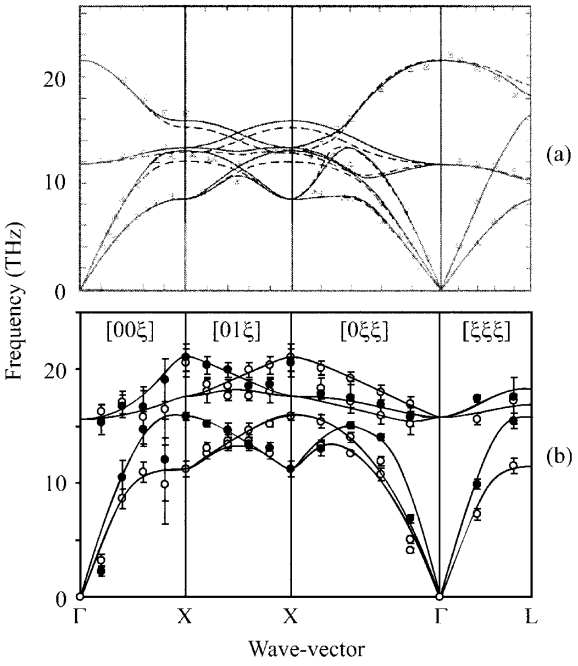

FIG. 1. (a) MgO phonon dispersion curves from INS experiments [17] (data points) and calculated using a shell lattice dynamical model [13] (solid lines). (b) Our analysis of RMC configurations derived from NPD data. The filled circles correspond to modes with predominantly longitudinal character and the open circles to those with transverse character. The lines are guides to the eye; each traces data with similar eigenvectors.

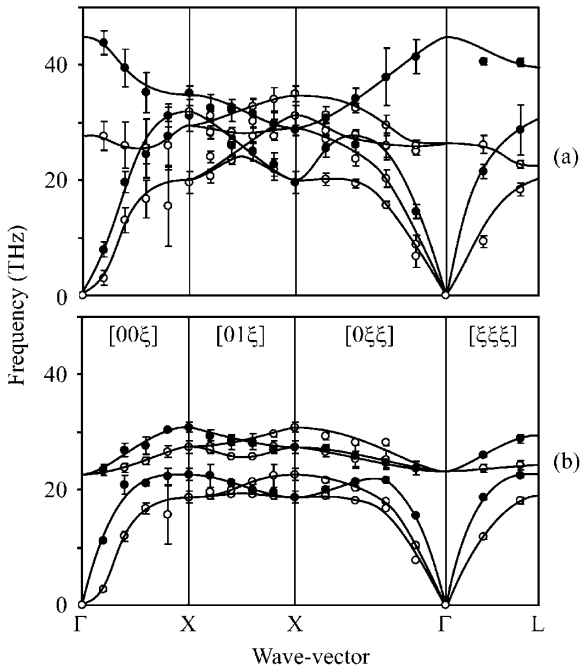

FIG. 2. MgO phonon dispersion curves from our analysis of (a) MD configurations and (b) RMC configurations refined against MD-derived diffraction data. The filled circles correspond to modes with predominantly longitudinal character and the open circles to those with transverse character. The lines are guides to the eye; each traces data with similar eigenvectors.

subtle effect to be extracted from atomic displacements alone.

To determine whether the absence of LO/TO splitting was a limitation imposed by the level of dynamics information contained within the diffraction data or whether it was a product of our method of analysis, we generated a new ensemble of atomistic configurations using MD. The model used was a standard shell potential, which is capable of reproducing LO/TO splitting at the zone center [16]. We performed MD calculations on a configuration containing a $5 \times 5 \times 5$ array of fcc unit cells. To approach the same statistics observed with phonon analysis of RMC-generated configurations, we required 3000 of these MD-generated configurations. The resulting phonon dispersion curves observed (using the above approach) are illustrated in Fig. 2(a). The difference in absolute energies between these curves and those illustrated in Fig. 1 is relatively unimportant as it merely reflects the choice of parameters used in the potential model. On the other hand, the presence of LO/TO splitting at the zone center indicates that it is not the method of phonon analysis itself that is responsible for the loss of this feature in the RMC-derived phonon dispersion curves.

As a rigorous test of this conclusion, we generated artificial $S(Q)$, $T(r)$, and Bragg intensity data sets from the MD configurations and subsequently used these as input for the RMC procedure. A further 500 configurations were generated in this manner, using precisely the same parameters used initially to generate configurations from the experimental diffraction data. Again, each configuration contained a $5 \times 5 \times 5$ array of fcc unit cells. These configurations exhibit essentially the same diffraction behavior as the MD configurations (in the absence of experimental "noise", the RMC fits obtained were near perfect). However, our analysis yielded phonon dispersion curves, illustrated in Fig. 2(b), that lacked any observable splitting between the LO and TO branches at the zone center. The similarity in appearance to the curves obtained from the NPD experimental data [Fig. 1(b)] is striking.

Finally, we considered the possibility that the similarity in the scattering lengths of Mg and O ($b = 5.375, 5.803$ fm, respectively) was responsible for the lack of splitting, given that the Mg and O sites are crystallographically identical. By exploiting our collection of MD-derived configurations, we were able to generate artificial $S(Q)$, $T(r)$, and Bragg intensity data sets using arbitrary scattering lengths for Mg and O atoms. Even assigning scattering lengths of different sign had minimal effect on the observed phonon dispersion. In particular, it did not restore the LO/TO splitting at the zone center.

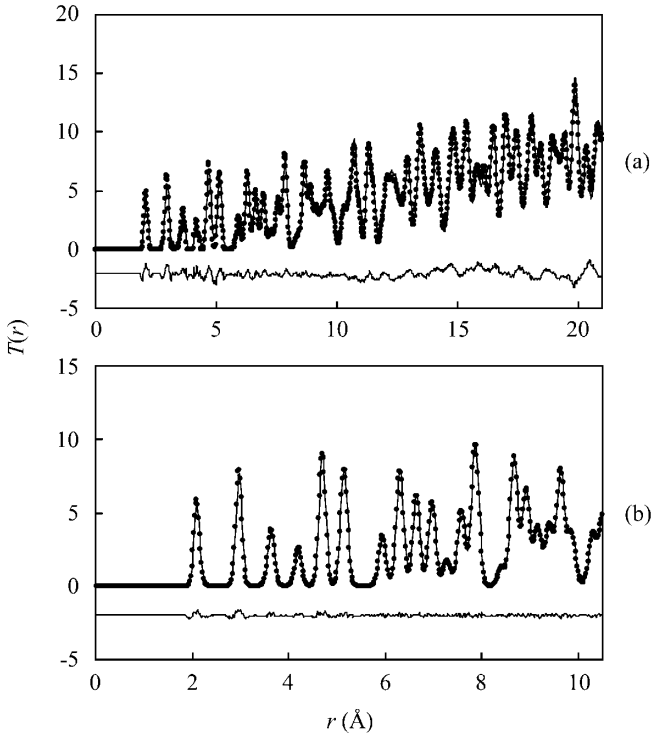

FIG. 3. RMC refinement of (a) neutron diffraction and (b) molecular dynamics $T(r)$ data. The dots are the experimental values and the solid lines are calculated from the refined RMC structural models described in the text. The lower trace in each plot shows the difference (measured − calculated), offset vertically by −2. The range of r values differs between plots as a consequence of the corresponding difference in configurational box size.

The experimental and RMC-modeled radial distribution functions $T(r)$ for both the NPD-derived and MD-derived data sets are illustrated in Fig. 3. Significantly, the "experimental" and modeled $T(r)$ curves for the data derived from MD calculations [Fig. 3(b)] are essentially indistinguishable. This is particularly intriguing given the dramatic difference in their corresponding phonon dispersion curves described above. The $T(r)$ data appear to be ignorant of the presence or absence of LO/TO splitting near the zone center.

In conclusion, our results have established that it is possible to extract relatively complex and valuable dynamics information from powder diffraction data of nontrivial systems. Furthermore, we have quantified the extent to which powder diffraction preserves such information. Atomic displacements due to high-frequency modes, such as the LO and TO branches in MgO, will be small in magnitude and hence their effect on functions such as the PDF will be subtle. However, reliable information regarding low-frequency modes (which tend to be the more relevant features when using dynamics to understand many physical properties of materials) is readily accessible using this approach, allowing investigation of the dynamics of many systems for which established methods are prohibitive or inappropriate.

We acknowledge support from the EPSRC (UK) and from Trinity College, Cambridge to A. L. G. We are grateful to Dr. Kostya Trachenko for his assistance with the MD simulations.

*Electronic address: martin@esc.cam.ac.uk

[1] M. Schwoerer-Bohning, A. T. Macrander, and D. Arms, Phys. Rev. Lett. **80**, 5572 (1998).
[2] T. Ruf, J. Serrano, M. Cardona, P. Pavone, M. Pabst, M. Krisch, M. D'Astuto, T. Suski, I. Grzegory, and M. Leszczynski, Phys. Rev. Lett. **86**, 906 (2001).
[3] D. A. Dimitrov, D. Louca, and H. Röder, Phys. Rev. B **60**, 6204 (1999).
[4] W. Reichardt and L. Pintschovius, Phys. Rev. B **63**, 174302 (2001).
[5] M. J. Graf, I.-K. Jeong, D. L. Starr, and R. H. Heffner, Phys. Rev. B **68**, 064305 (2003).
[6] I.-K. Jeong, R. H. Heffner, M. J. Graf, and S. J. L. Billinge, Phys. Rev. B **67**, 104301 (2003).
[7] M. G. Tucker, D. A. Keen, and M. T. Dove, Mineral. Mag. **65**, 489 (2001).
[8] To some extent, the details of the phonon dispersion curves in a material such as quartz are constrained by features of the structure, particularly by the fact that the low-energy excitations are those in which the atoms can move without giving rise to significant distortions of the tetrahedra, namely, the rigid unit modes. The patterns of diffuse scattering are directly determined by the distribution of the rigid unit modes across the BZ. We anticipated that some features of the dispersion curves of any material will be determined by structural constraints, with the diffraction data providing the energy scale via quantities such as the mean squared atomic displacements.
[9] M. G. Tucker, M. T. Dove, and D. A. Keen, J. Appl. Crystallogr. **34**, 630 (2001).
[10] D. A. Keen, J. Appl. Crystallogr. **34**, 172 (2001).
[11] M. T. Dove, *Introduction To Lattice Dynamics* (Cambridge University Press, Cambridge, England 1993).
[12] M. T. Dove, and R. M. Lynden-Bell, Philos. Mag. B **54**, 443 (1986).
[13] M. J. L. Sangster, G. Peckham, and D. H. Saunderson, J. Phys. C **3**, 1026 (1970).
[14] Alex. C. Hannon, The General Materials Diffractometer http://www.isis.rl.ac.uk/disordered/gem/gem_home.htm
[15] The resolution of the phonon dispersion curves is determined by the size of the configurational box size. In this instance, the $10 \times 10 \times 10$ supercell allows a maximum normalized k-resolution of 1/10. Intervals of 1/5 were chosen for Fig. 1 so as to facilitate comparison with the MD results shown in Fig. 2.
[16] G.V. Lewis and C. R. A. Catlow, J. Phys. C **18**, 1149 (1985).
[17] G. Peckham, Proc. Phys. Soc. London **90**, 657 (1967).